Magnetic information in the light diffracted by a negative dot array of Fe

P. Vavassori, V. Metlushko, R. M. Osgood III, M. Grimsditch, U. Welp, and G. Crabtree
Materials Science Division, Argonne National Laboratory, Argonne, Illinois 60439-4845

Wenjun Fan and S. R. J. Brueck
University of New Mexico, Albuquerque, New Mexico 87131

B. Ilic and P. J. Hesketh
Electrical Engineering and Computer Sciences, University of Illinois at Chicago, Chicago, Illinois 60607
(Received 20 August 1998; revised manuscript received 12 November 1998)

We have investigated the magnetic properties of an array of holes in an Fe film using the magneto-optic Kerr effect. We develop the theory of diffraction from an array to include magneto-optic effects. The theory allows us to interpret the differences in the magnetic loops observed on the reflected beam and those observed on diffracted spots. The latter contain more detailed information on the magnetic structure in the vicinity of the holes and allow us to infer differences in the switching mechanism for fields applied along the easy and hard axes. [S0163-1829(99)01509-X]

INTRODUCTION

During the last few years it has become possible to produce periodic arrays of submicron structures in metallic and superconducting films thanks to the precise control of microstructure offered by modern photolithography.[1–6] Tailoring with great precision size, period, and symmetry of the microstructures enables the fabrication of systems of potential technological interest.

Much of the interest arises from the possibility of fabricating nanoscale periodic structures of hybrid magnetic and superconducting materials[7] for optical and magnetic storage applications. For these applications the aim is to create periodic arrays of defects (such as submicron-sized holes) that act as pinning sites which enable control of the critical current of superconductors.[8] Although the investigation of the properties of arrays of magnetic dots has received some attention,[9–11] there have been very few studies on the reverse geometry, i.e., an array of nonmagnetic regions defined within a magnetic thin film,[12,13] these systems have become known as ''negative dots'' or ''antidots.''

In this paper we report on the magnetic properties of a 400 Å thick polycrystalline Fe film with a square array ($\approx 2\ \mu$m$\times 2\ \mu$m lattice constant) of submicron circular holes (radius of $\approx 0.2\ \mu$m) defined on the film by interferometric photolithography. By means of the transverse magneto-optic Kerr effect we studied the switching process of the magnetization in the film in the regions with and without holes. The results indicate that, for the array spacing investigated, the coercive field and anisotropy of the film are only slightly influenced by the holes. We show, however, how it is possible to obtain information on the switching mechanism of the magnetization in a more restricted area around the dots exploiting the information contained in the diffracted beams. A different switching mechanism when the field is applied along the hard and easy axes is traced to the peculiar domain structure around the holes.

EXPERIMENTAL SETUP

The sample was prepared on a Si (100) substrate using interferometric lithography and dc magnetron sputtering. A complete description of the sample preparation will be published elsewhere.[14] Briefly, the desired pattern was defined on a photoresist layer by the interference pattern created by two coherent, equal-intensity plane waves derived from a single laser source ($\lambda = 364$ nm from a TEM_{00} Ar-ion laser). After the development process an array of photoresist pillars, suitable for the subsequent liftoff step, remains on the Si surface. Using dc magnetron sputtering a 400-Å-thick polycrystalline Fe film is deposited onto the array of photoresist pillars. These are then dissolved, and the film containing a square array of holes is obtained. Our sample is a 400-Å-thick polycrystalline Fe film in which a $d \approx 2\ \mu$m$\times 2\ \mu$m square array of circular holes, with an average radius $a \approx 2000$ Å, has been defined. An atomic-force microscopy (AFM) image, recorded on the patterned half of the film, is shown in Fig. 1. The image clearly shows the square 2×2 micron hole array and the circular holes. It also shows that each hole is surrounded by an unwanted ridge; the origin of this ridge could, in principle, be either remnant photoresist or Fe which was deposited on the pillar walls. Based on the results of repetitive etching of other nanostructures we believe that the ridges are still due to remnant photoresist. This conclusion is indirectly corroborated by our magnetic force microscopy (MFM) images, which show very little evidence of the hole pattern. Since MFM is sensitive mainly to the perpendicular field, this is not too surprising since the magnetization lies in the plane of the sample. However if the holes did have Fe ridges we would expect these ridges to produce an enhanced perpendicular field; their absence is an indication that, even if present, the ridges have little effect on the magnetization direction. The patterned area covers only a half of the film surface; this allows a straightforward comparison between the magnetic behavior of the Fe film with and without the pattern.

We have investigated the array and the nonpatterned areas

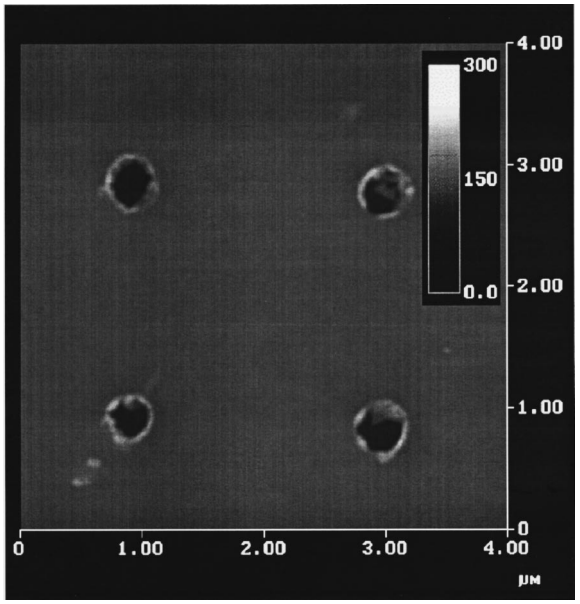

FIG. 1. AFM image of our patterned Fe film. The units of the height scale shown in the inset are nm.

of the film using the magneto-optic Kerr effect (MOKE). Superconducting quantum interference device (SQUID) magnetometry and Brillouin scattering were also used but, since they essentially confirmed the conclusions reached from the MOKE results, they will be discussed only briefly.

The MOKE experiments allowed us to measure the components of the magnetization **M** in the film plane parallel and perpendicular to the applied field **H**. The external field was either in the plane of incidence or perpendicular to it and was always in the plane of the sample. The measurements discussed here were made in the transverse Kerr effect configuration[15] with *p*-polarized incident light (E in the plane of incidence) and applying the external field **H** normal to or in the plane of incidence to obtain the components of **M** parallel and perpendicular to **H**, respectively. The angle of incidence θ of the light was set to $\theta \approx 45°$ with respect to the normal of the sample surface. In this article we refer to the components of **M** parallel and perpendicular to **H** as longitudinal (M_l) and transverse (M_t), respectively; this should not be confused with the often-used nomenclature of longitudinal and transverse Kerr effect.[15]

When the light was incident on the array of holes, the lateral periodicity of the array produced a two-dimensional diffraction pattern. We have performed MOKE measurements also on the diffracted light spots. Similar experiments have been reported for an array of square patches.[16]

THEORY

The conventional MOKE (Ref. 17) theory, since it implicitly contains the conditions appropriate for reflection geometry, is difficult to generalize to the case of diffracted light. We have found that it is convenient to visualize the patterned film as the superposition of two virtual samples, see Fig. 2, one continuous with a electric susceptibility χ (with χ that of Fe), and another composed of dots with reversed magnetization and susceptibility $-\chi$. In an electric field (E) such a combination clearly behaves like the original film with an

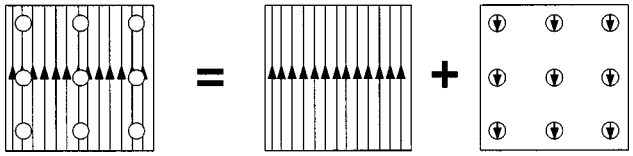

FIG. 2. Model of our patterned sample as two virtual films, one continuous, the other consisting of dots with reversed magnetization and negative susceptibility.

induced dipole moment χE everywhere except in the holes where it is zero. The advantage of the above description is that for diffracted spots only contributions from the ''dot'' sample need be considered. One immediate result is that the intensity of the diffracted spots is determined by the form factor (f) of a flat disk, viz.

$$f = \int_S e^{-i\mathbf{r}\cdot\Delta\mathbf{k}} ds = \int_S r e^{-irG\cos\alpha} dr\, d\alpha. \tag{1}$$

Here S is the negative dot surface, **r** is the position vector inside the hole, $\Delta\mathbf{k}=\mathbf{G}$ is the exchanged momentum, equal to a vector in the reciprocal hole lattice space, and α is the angle between **r** and $\Delta\mathbf{k}$. The integral is proportional to the $(1/G)*J_1(aG)$ where J_1 is the Bessel function, a is the hole radius and the resulting intensity is then predicted to be proportional to $[(1/G)*J_1(aG)]^2$.

To derive the magnetic contribution from each dot we simply write $\chi_{ij}=\chi_{oij}+K_{ijk}M_k$, where M_k is the k component of the magnetization (second-order terms in M_kM_j are negligible) and K_{ijk} is the magneto-optic tensor. We choose the coordinate system with the z axis along the surface normal, and the y axis perpendicular to the scattering plane.

Calling θ the angle that the incident laser beam makes with the z axis, the two principal polarizations of the incident laser beam (inside the film) are given by $e_1=(010)$ and $e_2=(1,0,\sin\theta/\sqrt{\varepsilon})$, where ε is the dielectric constant of Fe. The dipole moment induced in the Fe film is then given by $e_i\cdot\chi$. The diffracted intensity, analyzed in polarization $e_{\mathbf{k}}$, is

$$I \quad \alpha \quad |e_i\cdot\chi_{ik}\cdot e_k|^2, \quad i \text{ and } k=1,2. \tag{2}$$

From Eq. (2) we can easily obtain the expected MOKE signals originating from the variations in χ caused by changes in the magnetization. These can be written as

$$\Delta\chi = K\begin{bmatrix} 0 & M_z & -M_y \\ M_z & 0 & M_x \\ M_y & -M_x & 0 \end{bmatrix}. \tag{3}$$

Because of the complications in the polarization of the scattered beam when dealing with diffracted spots away from the scattering plane[18] we report here only Kerr loops obtained on diffracted spots lying in the plane. Indicating the polarizations as $s=(0,1,0)$ (perpendicular to the scattering plane) or $p=(-\cos\phi,0,\sin\phi)$ (in the scattering plane, where ϕ is the angle between the diffracted beam and the z axis), and using subscripts and superscripts to indicate incident and scattered light; it turns out that the only polarization combination giving a signal proportional to the magnetization is the p polarization for both the incident and scattered light. In that case, keeping only linear terms in M_i, we have

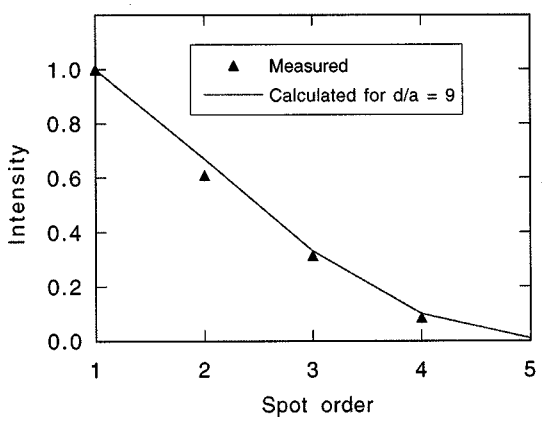

FIG. 3. Intensity of diffracted spots normalized to the intensity of the first-order spot for the sample at an angle $\omega=0°$ about the sample normal, with ω defined in Fig. 4. The triangles are experimental data, the full line is a fit as described in the text.

$$I_p^p=\left|2\chi_0 K M_y\left[\sin\phi\cos\phi+\frac{\sin\theta}{\sqrt{\varepsilon}}(\cos^2\phi-\sin^2\phi)-\frac{\sin^2\theta}{\varepsilon}\sin\phi\cos\phi\right]\right|^2. \tag{4}$$

The terms in Eq. (4) that contain ε are small and produce only a small variation of I_p^p for the values of ϕ corresponding to different diffraction spots. In all the other polarization combinations, namely I_p^s, I_s^p, and I_s^s, the intensity is proportional to terms second-order in M_i.

The magnetization loops, to be described in the next section, have been analyzed using Eq. (4). By applying the field along y (perpendicular to the plane of incidence) we have $\mathbf{M_y}=\mathbf{M_l}$, while when $\mathbf{H}$ is along x (in plane) $\mathbf{M_y}$ of Eq. (4) corresponds to $\mathbf{M_t}$.

We point out that the above analysis does not predict a change in the shape of the Kerr loop when changing the order of the diffraction spot. Since this is in apparent contradiction with the results presented in Ref. 16 on magnetic dots, we note that in that case the changes with diffraction order were ascribed to domain structure within each dot. In our analysis we would have to include magnetic structure within each dot in order to induce structure into the form factor. Since our experimental results show no obvious dependence on diffraction order, we do not include such effects in our analysis.

RESULTS AND DISCUSSION

Diffracted spot intensities

In Fig. 3 we plot the measured intensities (triangles) of the successive diffracted spots for the sample at an angle $\omega=0°$ about the sample normal, with ω defined in Fig. 4. These have been fitted to $[(1/n)*J_1(naG)]^2=[(1/n)*J_1(2\pi na/d)]^2$ where n is the order of the diffracted spot and a/d, which is the fitting parameter, is the ratio between the radius of the holes and the interhole distance (a and d, respectively). The line shown in Fig. 3 corresponds to $a/d=1/9$ which is consistent with the interhole distance that can be estimated from the AFM image of Fig. 1 (d is in the range 1.8–2.0 μm and $a\approx 0.2\,\mu$m).

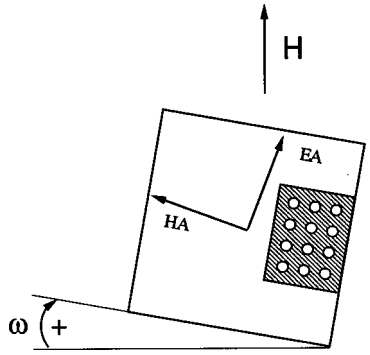

FIG. 4. Schematic view of our sample rotation showing the orientation of the hard and easy axes.

The good agreement between the measurements and the theory provides some justification for the approach of treating the sample as two virtual films as shown in Fig. 2. The rigorous mathematical justification for this approach is discussed in more detail in Ref. 19.

Nonpatterned Fe film

For different angles of rotation ω about the sample normal, with ω defined in Fig. 4, the $\mathbf{M}_l$ and $\mathbf{M}_t$ loops measured for the nonpatterned film are shown in Fig. 5. It is evident from the different shape of the loops that the continuous film exhibits an in-plane anisotropy. The $\mathbf{M_t}$ vs $\mathbf{H}$ loops indicate that $\mathbf{M}$ reverses mainly by coherent rotation and not by domain formation. A comparison of the loops also shows the

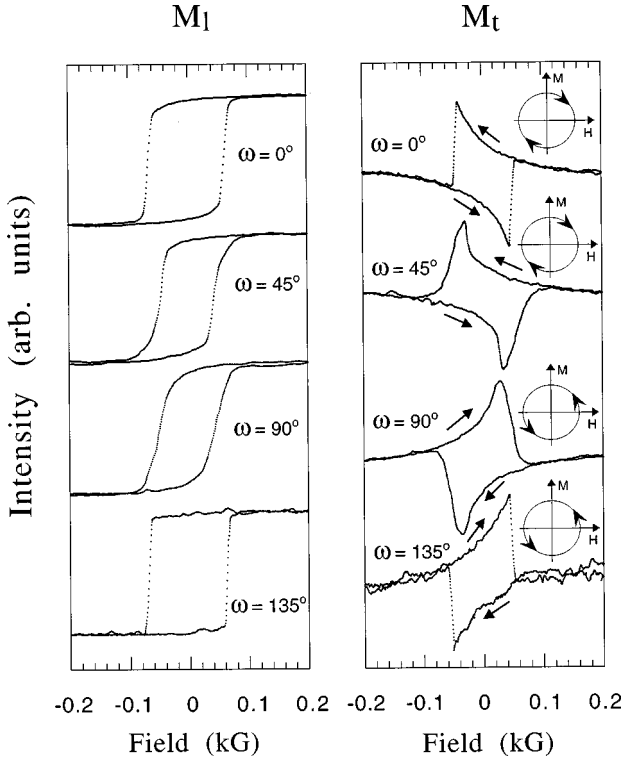

FIG. 5. MOKE loops of longitudinal (M_l) and transverse (M_t) components of the magnetization on the nonpatterned film as a function of sample rotation.

presence of a uniaxial easy axis at an angle ω between 135° and 180° as indicated schematically in Fig. 4. The existence of hard and easy axes can be seen from the fact that $\mathbf{M_t}$ vs $\mathbf{H}$ loops show that $\mathbf{M}$ undergoes a change in the sense of rotation, from clockwise to counterclockwise as sketched in Fig. 5, when ω goes from 0° (equal to 180°) to 135°, respectively. Consistently both the $\mathbf{M_l}$ and $\mathbf{M_t}$ vs $\mathbf{H}$ loops at 0° and 135° show an abrupt ''jump'' of $\mathbf{M}$ when $\mathbf{H}$ exceeds a threshold value. The more rounded shape of the other loops (45° and 90°) shows that $\mathbf{M_l}$ rotates smoothly when $\mathbf{H}$ is swept along these directions. The above behavior is also reflected in the shape of the 45 and 90° $\mathbf{M_t}$ vs $\mathbf{H}$ loops which display a continuous rotation of $\mathbf{M}$ and a change in the sense of rotation indicating that there is hard axis between 45° and 90°; this is also sketched in Fig. 4. Because the $\mathbf{M_t}$ vs $\mathbf{H}$ loop at 90° shows a smoother rotation of $\mathbf{M}$, we conclude that the hard axis is closer to 90° than to 45°. We attribute the anisotropy in the nonpatterned Fe polycrystalline film to a strain anisotropy induced during deposition. In fact, in the geometry adopted for the film deposition, the sputtering source is at an angle of about 20° degrees with respect to the substrate normal. To conclude we note that the loops show a larger coercive field for the easy-axis loops as compared with the hard axis as expected for a rotational model with uniaxial anisotropy.

Patterned Fe film: reflected spot

As discussed in the Theory section we expect the magnetoptic signal in this beam to be the superposition of the contribution from a uniform film plus that from the dots with reversed magnetization. Since, based on a total area argument, the former is expected to be larger we expect the signal to be the same as that from the nonpatterned area.

The loops measured in this case are shown in Fig. 6. The small differences observed when comparing these loops with those for the continuous film, indicates that the presence of the holes modify only slightly the sample's anisotropy and coercivity. This result is in agreement with that reported in Ref. 12 for a similar hole array density in Permalloy, even though in that case the diameter of the holes was of about 100 μm. Only small differences are observable in the coercivity and in the shape of some loops. The former shows a small increase of its value with respect to the nonpatterned film for the ''hard-axis'' loops (from 45 to about 52 G). Small differences in shape are also observable for the ''hard-axis'' loop at 90°; it shows a sharper transition (higher slope of $\mathbf{M}$ for $\mathbf{H}$ around the coercive field) while the rotation of $\mathbf{M}$ approaching the saturation is more gradual. Slight shape changes are also observable in the $\mathbf{M_t}$ vs $\mathbf{H}$ loops that show a sharper peak followed by slower decrease with respect to the film. These changes could be due to a small modification of the anisotropy induced by the square hole lattice or to the contribution from the negative dots to be discussed below. Further investigations on samples with more closely packed holes are needed to resolve these subtle changes.

SQUID and Brillouin measurements

We have also carried out room-temperature SQUID measurements on the patterned region, measuring both $\mathbf{M}_l$ and $\mathbf{M}_t$ as function of the external field. (These experiments, which required breaking the sample, were performed after all MOKE experiments were completed). The results confirm the existence of easy and hard axes and the switching mechanism. We also performed Brillouin light-scattering experiments for different rotation angles of the sample, and from both the nonpatterned and patterned regions. The magnons frequency shifts vs external field show the same behavior in the two regions, indicating that neither the anisotropy nor the magnetization is appreciably modified by the array of holes.

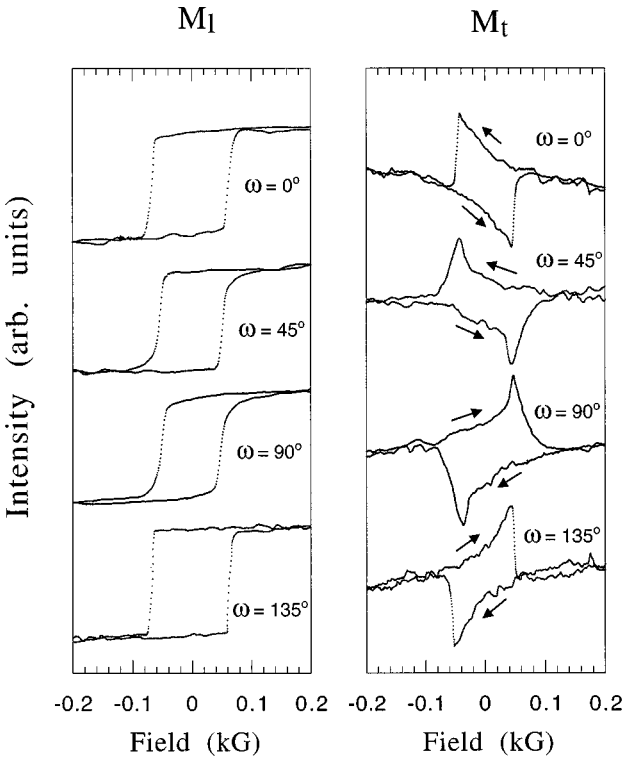

FIG. 6. Angle dependence of MOKE loops of longitudinal (M_l) and transverse (M_t) components of the magnetization measured on the reflected spot from the patterned portion of the film.

Patterned Fe film: diffraction spots

Based on the theory described in the previous section, i.e., treating the holes as dots with reversed magnetization, the MOKE signal on a diffracted spot should be identical to that in the reflected spot.

The loops measured analyzing the light coming from a diffraction spot of order $n=1$ lying in the plane of incidence are shown in Fig. 7. The general behavior of the loops is the same as that reported above: the anisotropy is unchanged with respect to the continuous and patterned film and the coercivity is almost the same as that observed on the patterned area. The only new features are the presence of a wiggle in the $\mathbf{M_l}$ vs $\mathbf{H}$ hard-axis loops and a double step in the corresponding $\mathbf{M_t}$ vs $\mathbf{H}$ loops. These features are perfectly reproducible and are observed in the vicinity of the switching of the magnetization direction.

A priori the most likely explanation for the additional features would seem to be higher-order contributions to the magneto-optic signal. A strong argument against this explanation is that, if it were correct, there is no obvious reason why it should not contribute to the signal from the nonpat-

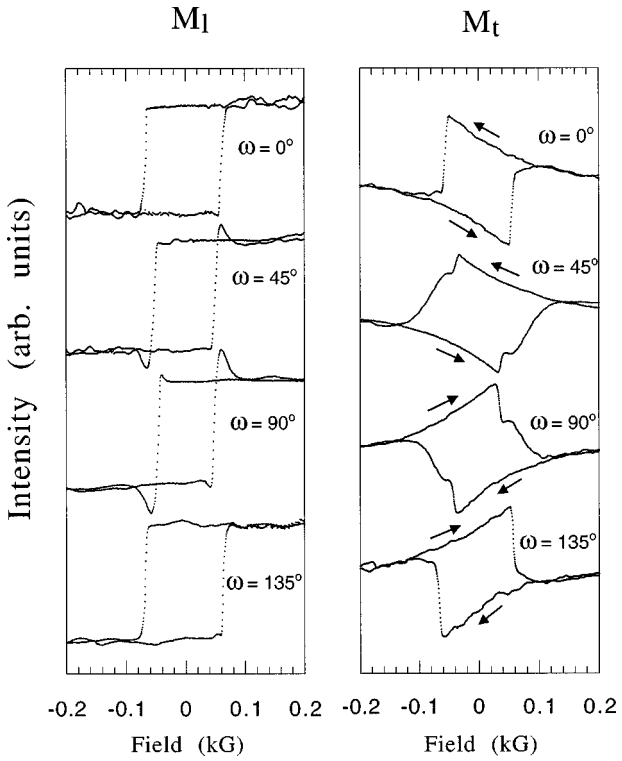

FIG. 7. As in Fig. 6 but with the MOKE loops measured on a diffracted spot from the patterned portion of the film.

terned film. This explanation can, however, also be discounted by more direct arguments. Following the treatment of the distortions in the magneto-optic loops due to second-order terms as given in Ref. 20, the quadratic terms can be ruled out for the following reasons:

(i) The decreasing side of the wiggles in the $\mathbf{M}_l$ loops is inconsistent with an $\mathbf{M}_l^2$ contribution since the latter should not decrease.

(ii) The $\mathbf{M_l M_t}$ contributions to the loops should have mirror symmetry with respect to the **M** and **H** axes and create an asymmetry in the magneto-optical hysteresis loop (Ref. 20 and references quoted therein). On the contrary, our loops possess inversion symmetry about the origin.

(iii) The intensity of the wiggles do not vary by changing the angle of incidence (between 45° and 15°), while the contributions of second-order effects are expected to be larger at small angles of incidence.

(iv) Estimates of the intensity of the quadratic terms indicate that they should be considerably smaller than that of the linear terms.

Having ruled out quadratic contributions we have concluded that the distortions are related to the behavior of **M** in the vicinity of the holes. The appearance of domains can give rise to interference effects that distort the diffraction loops.[16] These distortions, as previously mentioned, are related to the n/d Fourier component of the spatial distribution of **M**. In general, differently shaped diffraction loops could be expected by changing n. However, experimentally we found that the shape of the diffraction loops do not change [apart from the overall intensity as predicted by Eq. (4)] when changing the order n of the diffracted spot analyzed. The stability in the shape of the loops implies that the spatial

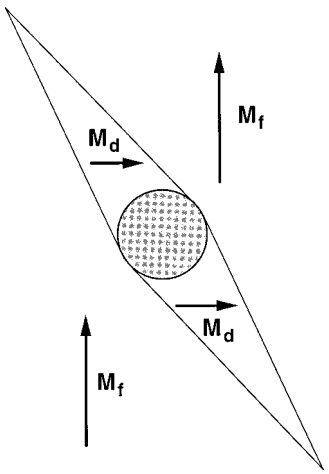

FIG. 8. Schematic diagram of blade domains relative to a hole.

distribution of the magnetization around the holes has the same lateral periodicity of the array.

When a hole is present in a ferromagnetic material the surface energy contributions are large. It is known[21] that in such situations domains, with **M** at 90° with respect to the rest of the sample can be induced so as to reduce the magnetostatic energy. Due to the energy minimization, these domains are expected to have a blade shape, as shown in Fig. 8, and this indeed is the shape of the domains observed around voids and inclusions in ferromagnetic films reported in literature.[21] Although, the detailed shape of these domains is not essential in our discussion. For ease of presentation we assume that if domains form around the holes they will be blade shaped. Since domain formation competes with the anisotropy of the film, their formation may be inhibited (favored) when their magnetization is oriented along the hard (easy) axis.

The existence of such domains should have two effects: it should change the coercivity and the shape of the loops, as pointed out above. Furthermore, since the domains will form more easily when the film is magnetized along the hard axis, we may expect the hard-axis loops to show larger effects; this is indeed consistent with our observations.

The most straightforward indication that domains are present is in the $\mathbf{M_t}$ loops in Fig. 7. Here the double step is consistent with the formation of domains; the slow rise in $\mathbf{M_t}$ corresponds to the gradual rotation of the magnetization of the film, then, when the magnetization approaches its switching point, the domains are formed and they lead to the extra signal that gradually reduces as the field increases. Based on energy considerations it can be seen that the magnetization of the domains must point in the opposite direction with respect to the $\mathbf{M_t}$ component caused by the rotation of the magnetization of the film, so that the domain signal subtracts from the rotational $\mathbf{M_t}$ leading to the double step shape in the diffraction loop. This is shown in Fig. 9(a) for the hard-axis transverse loops at 90°, where we used the loop measured on the reflected spot to represent the $\mathbf{M_t}$ due to the rotation of film magnetization [line (a) in Fig. 9]. The difference signal between line (a) and the $\mathbf{M_t}$ loop from the diffraction spot [line (b)], is a peak with a sharp rise during the switching of the magnetization and a gradual decrease as the field increases further. This is consistent with the rapid formation of

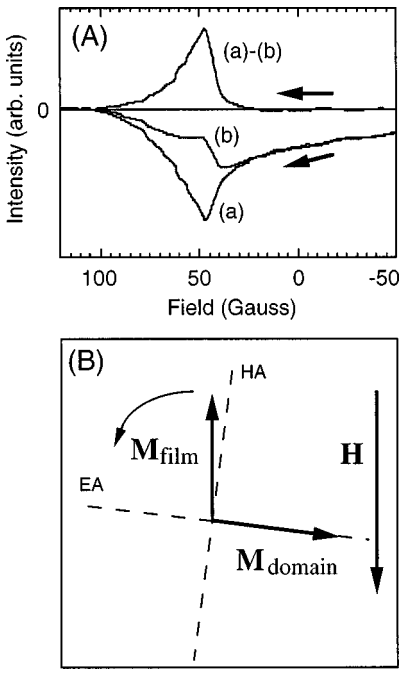

FIG. 9. (a) MOKE loops of transverse component of the magnetization from the 90° rotated sample from reflected (curve a) and diffracted spots (curve b). The upper curve is their difference and represents the contribution from the domains. (b) Diagram of sample showing why the blade domain contribution to M_t is opposite to that of the rotation.

the domains just before and during the switching and its gradual reduction at larger fields. The preferred orientation of the magnetization of the domains comes from the interplay between the directions of the easy axis and the external field, as shown in Fig. 9(b).

The wiggles in the $\mathbf{M}_l$ loops, however, have a slightly different explanation. The sample with domains can be viewed as the superposition of three virtual films as shown in Fig. 10: viz., the continuous film with its magnetization parallel to **H**, the holes and domain portions with the magnetization antiparallel to **H**, and the domain portions with the magnetization perpendicular to **H**. The continuous film (virtual film 1) has no contribution to the diffracted spots, and the domain regions (virtual film 3) contribute no signal to the longitudinal loop. The $\mathbf{M}_l$ loop therefore comes only from virtual film 2; because the active area of this film is larger when domains are present, the $\mathbf{M}_l$ signal is larger during the existence of domains. (In physical terms one must view this increase in signal as a loss of destructive interference in the

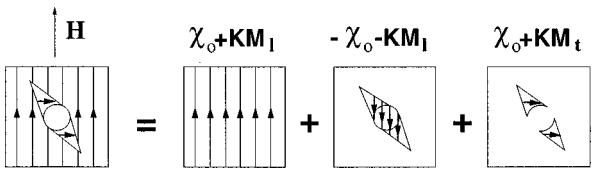

FIG. 10. Diagram of the three virtual films which can be envisioned as producing the observed loops in Fig. 7.

diffracted beam). We stress that the spatial distribution of the magnetization associated with the above described domains has the same lateral periodicity of the holes array (see Fig. 10) and, therefore, the shape of the loops are not expected to change with *n*. This is consistent with our observations and gives further evidence of the formation of domains around the holes. It is interesting to note that the intensity of the wiggles in Fig. 7 are ≈50% that of the 90° loop itself; this allows us to estimate the sampled area around the holes to be comparable to the holes themselves. In the case of the sample rotated by 45° the intensity of both the wiggles in the $\mathbf{M}_l$ loop and the step in the $\mathbf{M}_t$ loop are smaller than at 90°. This can be understood since, at this angle, the orientation of the easy axis is less favorable for formation of domains.

CONCLUSIONS

In this paper we report a magneto-optic study of the magnetic properties of a Fe film with a square array of submicron circular holes. The measurements carried out with the standard Kerr effect configuration indicate that the presence of the holes does not appreciably modify the sample's anisotropy or coercivity. We showed, however, how it is possible to obtain more detailed information on the magnetic structure in the vicinity of the holes from the diffracted light. To this purpose we developed a model to interpret the magnetic loops observed on diffracted spots. The model allowed us to infer differences in the switching mechanism for fields applied along the easy and hard axes.

ACKNOWLEDGMENTS

Work of Argonne National Laboratory was supported by the U.S. Department of Energy, Division of Material Sciences, Office of Basic Energy Sciences, under Contract No. W-31-109-ENG-38. We thank Dr. D. Hinks for providing the SEM characterization of the sample surface and C. H. Sowers for the Fe film deposition. P.V. acknowledges support by a research grant from INFM-Istituto Nazionale per la Fisica della Materia.

[1] H. Anderson, C. M. Horowitz, and H. I. Smith, Appl. Phys. Lett. **43**, 874 (1983).

[2] S. H. Zaidi, and S. R. J. Brueck, J. Vac. Sci. Technol. B **11**, 658 (1993); S. H. Zaidi, A.-S. Chu, and S. R. J. Brueck, J. Appl. Phys. **80**, 6997 (1996); X. Chen, S. H. Zaidi, S. R. J. Brueck, and D. J. Devine, J. Vac. Sci. Technol. B **14**, 3339 (1996).

[3] T. A. Savas, S. N. Shah, M. L. Schattenburg, J. M. Carter, and H. I. Smith, J. Vac. Sci. Technol. B **13**, 2732 (1996); A. Fernandez, J. Y. Decker, S. M. Herman, D. W. Phillion, D. W. Sweeney, and M. D. Perry, *ibid.* **15**, 2439 (1997).

[4] X. Chen, Z. Zhang, S. R. J. Brueck, R. A. Carpio, and J. S. Petersen, Proc. SPIE **3048**, 309 (1997).

[5] C. O. Bozler, C. T. Harris, S. Rabe, D. D. Rathman, M. A. Hollis, and H. I. Smith, J. Vac. Sci. Technol. B **12**, 629 (1994).

[6] A. Fernandez, H. T. Nguyen, J. A. Britten, R. D. Boyd, M. D. Perry, D. R. Kania, and A. M. Hawryluk, J. Vac. Sci. Technol. B **15**, 729 (1997).

[7] J. I. Martin, M. Velez, J. Nogues, and I. K. Schuller, Phys. Rev. Lett. **79**, 1929 (1997); D. J. Morgan and J. B. Ketterson, *ibid.* **80**, 3614 (1998).

[8] V. V. Metlushko, M. Baert, R. Jonckheere, V. V. Moshchalkov, and Y. Bruynseraede, Solid State Commun. **91**, 331 (1994); M. Baert, V. V. Metlushko, R. Jonckheere, V. V. Moshchalkov, and Y. Bruynseraede, Phys. Rev. Lett. **74**, 3269 (1995); V. V. Moshchalkov, M. Baert, V. V. Metlushko, E. Rosseel, M. J. Van Bael, K. Temst, R. Jonckheere, and Y. Bruynseraede, Phys. Rev. B **54**, 7385 (1996); V. V. Moshchalkov, M. Baert, V. V. Metlushko, E. Rosseel, M. J. Van Bael, K. Temst, Y. Bruynseraede, and R. Jonckheere, *ibid.* **57**, 3615 (1998); V. V. Metlushko, L. E. DeLong, M. Baert, E. Rosseel, M. J. Van Bael, K. Temst, V. V. Moshchalkov, and Y. Bruynseraede, Europhys. Lett. **41**, 333 (1998).

[9] C. Mathieu *et al.*, Appl. Phys. Lett. **70**, 2912 (1997); J. Appl. Phys. **81**, 4993 (1997).

[10] M. Grimsditch, Y. Jaccard, and I. K. Schuller, Phys. Rev. B **58**, 11 539 (1998).

[11] S. Wirth, J. J. Heremans, S. von Molnár, M. Field, K. L. Campman, A. C. Gossard, and D. D. Awschalom, IEEE Trans. Magn. **34**, 1105 (1998).

[12] C. A. Grimes, P. L. Trouilloud, J. K. Lumpp, and G. C. Bush, J. Appl. Phys. **81**, 4720 (1997).

[13] Y. Otani, S. G. Kim, T. Kohda, K. Fukamichi, O. Kitakami, and Y. Shimada, IEEE Trans. Magn. **34**, 1090 (1998).

[14] V. Metlushko, U. Welp, G. Crabtree, R. M. Osgood III, S. D. Bader, Zhao Zhang, S. R. J. Brueck, B. Watkins, L. E. DeLong, B. Ilic, K. Chung, and P. J. Hesketh, Phys. Rev. B **59**, 603 (1999).

[15] M. J. Freiser, IEEE Trans. Magn. **MAG-4**, 152 (1968).

[16] O. Geoffroy, D. Givord, Y. Otani, B. Pannetier, A. D. Santos, M. Schlenker, and Y. Souche, J. Magn. Magn. Mater. **121**, 516 (1993); Y. Souche, M. Schlenker, and A. D. Santos, *ibid.* **140**, 2179 (1995); Y. Souche, V. Novosad, B. Pannetier, and O. Geoffrey, *ibid.* **177**, 1277 (1998).

[17] See, e.g., G. Metzger, P. Pluvinage, and R. Torguet, Ann. Phys. (N.Y.) **10**, 5 (1965).

[18] R. M. Osgood III, S. K. Sinha, J. Freeland, Y. U. Idzerda, and S. D. Bader (unpublished).

[19] J. M. Cowley, *Diffraction Physics* (North-Holland, Amsterdam, 1975), pp. 47 and 48.

[20] R. M. Osgood III, S. D. Bader, B. M. Clemens, R. L. White, and H. Matsuyama, J. Magn. Magn. Mater. **182**, 297 (1998).

[21] S. Chicazumi and S. Charap, *Physics of Magnetism* (Wiley, New York, 1964); H. J. Williams, R. M. Bozorth, and W. Shockley, Phys. Rev. **75**, 155 (1949); L. Néel, Cah. Phys. **25**, 21 (1944).